Open Access Library Journal
2025, Volume 12, e13623
ISSN Online: 2333-9721
ISSN Print: 2333-9705

Signal Intensity Ratios and Anatomical Factors as Indicators of Anterior Cruciate Ligament Graft Healing: A 2-Year MRI Study

Erasme Ngendakumana[1], Abdoul Rachid Mahaman Mallam[1], Mengdong Wang[1], Ulrich Mizero[2], Jean Claude Nduwayezu[3], Siyu Chen[1], Xiaozhuan Wang[1], Dionys Nsanzabagenzi[4], Quan Zhou[1*]

[1]Department of Medical Image, Third Affiliated Hospital of Southern Medical University (Academy of Orthopedics, Guangdong Province), Guangzhou Guangdong
[2]Department of Orthopedic Surgery, Nanfang Hospital of Southern Medical University, Guangzhou Guangdong
[3]Department of Radiology, Zhujiang Hospital of Southern Medical University, Guangzhou, Guangdong
[4]Department of Nephrology, Zhujiang Hospital of Southern Medical University, Guangzhou, Guangdong
Email: *zhouquan3777@smu.edu.cn

How to cite this paper: Ngendakumana, E., Mahaman Mallam, A.R., Wang, M.D., Mizero, U., Nduwayezu, J.C., Chen, S.Y., Wang, X.Z., Nsanzabagenzi, D. and Zhou, Q. (2025) Signal Intensity Ratios and Anatomical Factors as Indicators of Anterior Cruciate Ligament Graft Healing: A 2-Year MRI Study. *Open Access Library Journal*, **12**: e13623.
https://doi.org/10.4236/oalib.1113623

Received: May 18, 2025
Accepted: August 9, 2025
Published: August 12, 2025

Abstract

Background: Prior studies have established that ACL graft healing is a prolonged process, which often lasts up to two years, with the MRI signal intensity ratio (SIR) serving as a key indicator of graft maturity. However, the factors influencing delayed healing, particularly anatomical variation, remain poorly understood. **Purpose:** To analyze magnetic resonance imaging changes in graft healing 2 years after anterior cruciate ligament reconstruction and identify independent factors associated with poor ACL graft healing. **Study Design:** Cross-sectional study. **Methods:** A total of 54 patients who underwent ACL surgery and had knee MRI examinations 2 years post-operation were included in the study; graft healing was assessed via MRI signal intensity ratios (SIRs) by dividing the mean graft signal by the PCL signal. The ITK-SNAP software was used to outline the boundaries of both the ACL graft and the fossa intercondylar femur and calculate the area of each layer automatically. Univariate and multivariate logistic regression models were created to evaluate independently correlated factors. **Results:** The mean SIR in the femoral aperture was significantly greater than that in the tibial aperture (3.70 ± 1.05 vs 2.70 ± 0.83, respectively, P = 0.001). Univariate regression analysis revealed several factors significantly associated with the proximal graft SIR, including a small fossa intercondylar femur (P = 0.001), a larger graft size (P = 0.033), and a large LCAPD/PTAPD ratio (P = 0.026). Multivariate regression analysis revealed two significant factors: the LCAPD/PTAPD ratio, which was associated with the proximal graft SIR (P = 0.009), and the femoral aperture graft SIR (P = 0.005), and the fossa inter-

condylar femur, which was associated with both the proximal graft SIR (P = 0.011) and the femoral aperture graft SIR (P = 0.009). **Conclusion:** Most grafts presented an increased signal intensity ratio, particularly in the femoral and proximal regions. Additionally, a larger LCAPD/PTAPD ratio and a small fossa intercondylar femur were identified as independent factors associated with delayed or poor graft healing.

Subject Areas

Orthopedic Surgery, Imaging and Nuclear Medicine, Sports Medicine, Clinical Research

Keywords

Anterior Cruciate Ligament Graft Healing, Magnetic Resonance Imaging Signal-Intensity Ratio, ACL Graft Rupture

1. Introduction

The conventional treatment for a complete rupture of the anterior cruciate ligament (ACL) is reconstruction of the torn ligament with an autograft or allograft tendon [1] [2]. Anterior cruciate ligament reconstruction (ACLR) aims to restore knee stability and normal knee function. This allows a safe return to activity and reduces the risk of reinjury [3]. The long-term objective of anterior cruciate ligament (ACL) reconstruction is to avoid subsequent osteoarthritis owing to instability [4]. However, the incidence of graft failure in this frequent surgical technique remains rather high, with some publications reporting failure rates of up to 13.3% [5].

Previous studies have reported different clinical and biological methods for assessing the healing phase of an ACL graft at various stages. Different imaging modalities, arthroscopies, and biopsies have been utilized clinically to detect changes in the tendon graft following ACL reconstruction. Magnetic resonance imaging has previously been utilized in preclinical [6] and clinical [7] research to assess ACL graft quality and related outcomes. In large animal studies, the combination of ACL graft size (a measure of tissue quantity) and signal intensity (a measure of tissue quality) assessed from specific MRI sequences was linked with the mechanical [6] [8] and histological qualities of the graft following ACL reconstruction [9].

Recently, interest in determining whether MRI can be used as a tool to detect graft healing after anterior cruciate ligament reconstruction, and to guide preinjury activities and sports has increased. Therefore, the use of graft signal intensity measurement methods in different regions of interest (ROIs) has increased. Signal intensity ratios (SIRs) and signal-to-noise quotients (SNQs) are common ways to express these measurements [3] [10]. SIR = ACL graft signal intensity/PCL signal intensity. A decrease in SIR indicates reduced water content and theoretically bet-

ter maturity and healing of the graft, and an increase in SIR for an ACL graft indicates higher water content, and delayed or incomplete healing [11]. Some studies have demonstrated a high SIR in the proximal and femoral aperture regions due to the different biological properties of these areas [10]. Some potential risk factors that impact graft healing outcomes have been identified in previous studies, including patient characteristics such as sex; anatomic features such as tibial slope and femoral notch size; and operative details such as graft type, size orientation, and fixation [12].

Despite advancements in technical procedures and the implementation of effective rehabilitation protocols for ACL reconstruction, there continues to be a lack of consensus among studies regarding the specific MRI findings and the exact timeline for individuals to safely return to their preinjury level of activity. The factors that impact graft healing remain unidentified.

The purpose of this study was to analyze the magnetic resonance imaging changes of graft healing 2 years after anterior cruciate ligament reconstruction and identify independent factors associated with poor ACL graft healing.

2. Materials and Methods

2.1. Study Design

The study was a retrospective observational analysis with the approval of the ethics committee of the Third Affiliated Hospital of Southern Medical University. The participant's data and information were anonymized and identified before analysis; therefore, no written informed consent was presented.

2.2. Population Study

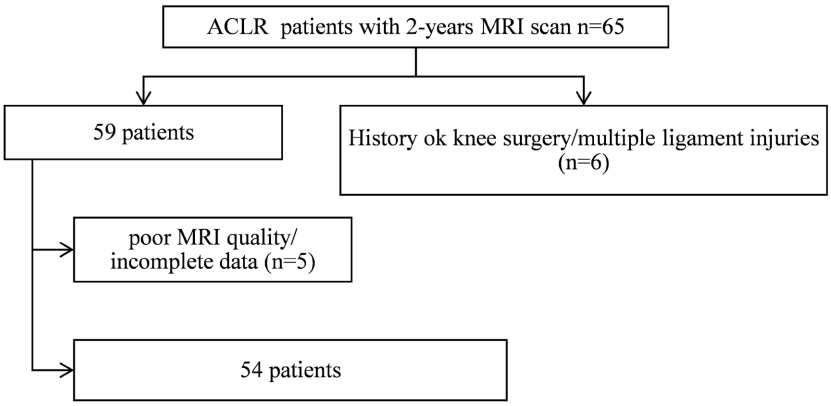

Figure 1. Patient recruitment flow diagram: anterior cruciate ligament reconstruction (ACLR) and magnetic resonance imaging (MRI).

The MR images of patients who underwent knee joint MRI scans for two years after surgery between January 2017 and December 2020 were obtained from the picture archiving and communication system (PACS) at Southern Medical University's Third Affiliated Hospital. This query was performed by a radiologist with years of clinical experience and diagnostic imaging skills. All subjects' DICOM MR vol-

umes were acquired via axial proton density-weighted spectral attenuated inversion recovery (PDW-SPAIR) sequences. Initially, 65 individuals of various ages were collected. Patients with a history of knee surgery were excluded to prevent confounding factors that could obscure the findings. Individuals with multiple-ligament injuries, incomplete data, or poor MRI image quality were also excluded. Finally, 54 individuals who fulfilled the inclusion and exclusion criteria were enrolled in this study (see **Figure 1**).

2.3. Surgical Technique

All patients underwent anterior cruciate ligament reconstruction using a hamstring autograft. The ACL remnant was removed via a 4 cm longitudinal incision medial to the tibial tubercle. The gracilis and semitendinosus tendons were combined to form a 4-strand graft, measured for optimal diameter (6.5 - 8.0 mm), and secured with an Endobutton. Femoral tunnels were drilled at the 10:30 position on the medial side of the lateral femoral condyle with dimensions of either 4.5 mm × 8 mm + Φ9.0 mm × 26 mm or 4.5 mm × 8 mm + Φ8.0 mm × 28 mm, at angles between 30˚ and 60˚ relative to the femur. Tibial tunnels were created with diameters of 9.0 mm or 8.0 mm at angles between 45˚ and 60˚ relative to the tibial. The graft was introduced through the tibial tunnel and tensioned by flexing and extending the knee 20 times, then fixed at the tibial end using a Biosure HA polylactic acid hydroxyapatite screw (9 mm × 30 mm or 8 mm × 30 mm).

2.4. Image Acquisition Protocol

A 3T MRI examination was performed at 2 years post-surgery of age via a dedicated unit (Magnetom Skyra, equipped with an 8-channel phased-array knee coil for both transmission and reception; Siemens AG Healthcare). The protocol included volumetric and nearly isotropic (0.5 mm × 0.5 mm × 0.65 mm) turbo spin echo sequences, which allowed for multiplanar reconstructions both parallel to the graft and perpendicular to the tunnel apertures [13]. An MRI scan was used as a surrogate to assess graft healing and integration. High-resolution 3-T MRI signal intensity ratios (SIRs), defined as the mean graft signal divided by the PCL signal [14], were estimated at regions of interest (ROIs) via oblique reconstructions parallel and perpendicular to the graft and tunnel apertures. The intra-articular graft was assessed via a sagittal oblique reconstructed image aligned parallel to the graft and three equal-spaced ROIs (proximal, middle, and distal), as reported in prior studies [15] [16]. A standardized 4 mm diameter circle was drawn around each area of interest (ROI), and the imaging software automatically calculated the average MRI signal intensity [17] [18].

The distal graft region of interest (ROI) was positioned directly proximal to the tibial aperture, with its distal border aligned with the tibial joint surface. The middle graft ROI was positioned so that its center was at the level of the anterior-distal intercondylar notch. The proximal graft ROI was placed next to the femoral ap-

erture, keeping the same distance as the distal and middle ROIs. The posterior cruciate ligament (PCL) signal was captured from an ROI near its base, which was centrally positioned relative to the broad distal connection on the tibia (**Figure 2(a)**).

The femoral and tibial aperture areas, as well as the graft signal intensity ratio (SIR), were measured with reconstructed images taken perpendicular to each aperture. The first slice with the tunnel walls entirely visible circumferentially was chosen for analysis. To determine the graft SIR, a circular region of interest (ROI) was defined throughout the tunnel. Furthermore, the area of this circle was used to estimate the tunnel area, and any tunnel widening was assessed by comparing this measurement to the tunnel size acquired during surgery (**Figure 2(b)**).

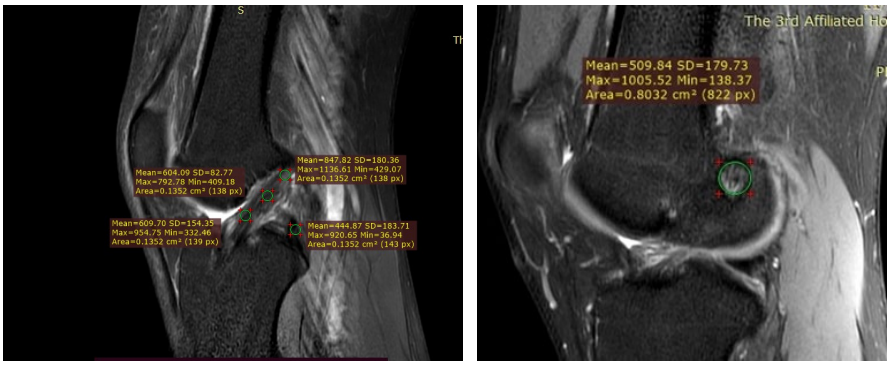

(a) (b)

Figure 2. (a) Final reconstruction to position regions of interest (ROIs) for the intra-articular graft. The image is parallel to the center of the graft. To determine the signal intensity ratio, 3 circular ROIs were positioned along the graft and at the root of the posterior cruciate ligament central to its broad tibial attachment. (b) Circular region of interest (ROI) for measuring the aperture area.

For notch volume measurement, all patients were scanned in the supine position using either a 1.5 T Achieva or a 3.0 T Ingenia MRI scanner, equipped with an eight-channel knee coil (Philips Healthcare, Best, Netherlands). The imaging parameters for the axial PDW-SPAIR sequence were as follows: field-of-view (FOV) = 160 mm × 160 mm × 92 mm, echo time (TE) = 30 ms, repetition time (TR) = 3000 ms, slice thickness = 4 mm, and flip angle = 90˚. The imaging parameters for the axFor notch volume measurement, all patients were scanned in the supine position using either a 1.5 T Achieva or a 3.0 T Ingenia MRI scanner, equipped with an eight-channel knee coil (Philips Healthcare, Best, Netherlands). The imaging parameters for the axial PDW-SPAIR sequence were as follows: field-of-view (FOV) = 160 mm × 160 mm × 92 mm, echo time (TE) = 30 ms, repetition time (TR) = 3000 ms, slice thickness = 4 mm, and flip angle = 90˚. The imaging parameters for the axial T_2-weighted SPAIR sequence were FOV = 160 mm × 160 mm × 105 mm, TE = 65 ms, TR = 2768 ms, slice thickness = 4 mm, and flip angle = 90˚. The axial slices (thickness of 4.0 mm and slice gap of 0.4 mm) were chosen to capture the femoral notch edges continuously, enabling the calculation of its vol-

ume. This approach was adapted from the methodology described by Zhang *et al.* T_2-weighted SPAIR sequence was FOV = 160 mm × 160 mm × 105 mm, TE = 65 ms, TR = 2768 ms, slice thickness = 4 mm, and flip angle = 90˚. The axial slices (thickness of 4.0 mm and slice gap of 0.4 mm) were chosen to continuously capture the femoral notch edges, enabling the calculation of its volume. This approach was adapted from the methodology described by Zhang *et al.* [19].

We used ITK-SNAP software (version 3.6; https://www.itksnap.org/pmwiki/pmwiki.php) to manually define the boundaries of each layer of the fossa intercondylar femur based on anatomical landmarks. The software automatically calculates the 2D area of the fossa for each layer. As shown in **Figure 3**, the most proximal limit of the intercondylar fossa was determined at the level where the femoral condyles and cartilaginous surfaces were clearly visible (**Figure 3(a)**). The most distal border was found at the final continuous layer of the condyle, where the femoral condyles remained anteriorly continuous (**Figure 3(c)**). **Figure 3(b)** shows one of the middle layers of the fossa intercondylar femur.

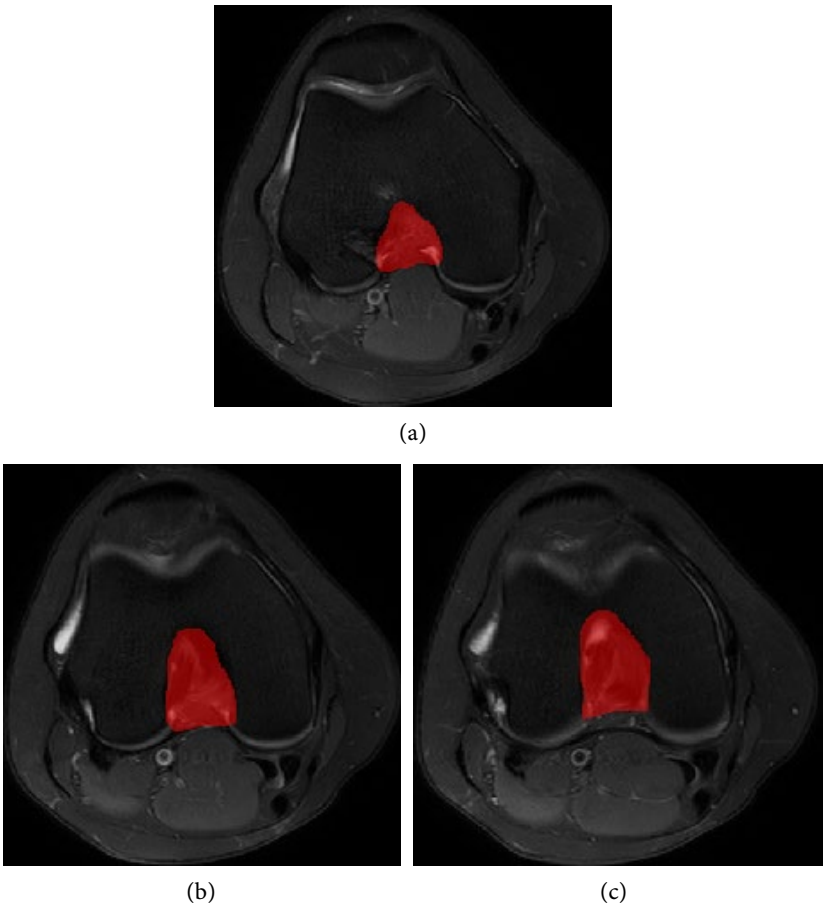

(a)

(b) (c)

Figure 3. Axial slices of knee MR image demonstrating the measurement of fossa intercondylar femur volume. (a) The fossa intercondylar femur at its most proximal position. (b) One of the middle layers of the fossa intercondylar femur. (c) Most distal level of the fossa intercondylar femur.

ITK-SNAP software was used to outline the ACL graft boundary and calculate the area of each layer automatically. The proximal tibia anterior-posterior distance (TPAPD) and lateral femoral condylar anterior-posterior distance (LCAPD) were measured via ITK-SNAP software (see Figure 4).

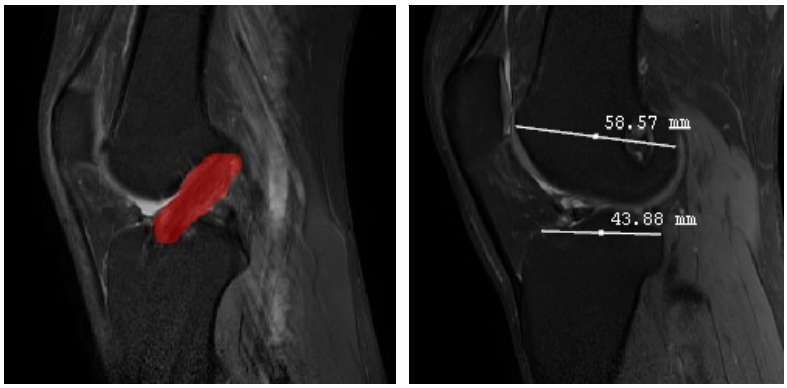

(a) (b)

Figure 4. (a) Graft volume = Area × Layer Thickness, (b) TPAPD and (LCAPD)/TPAPD ratio.

2.5. Statistical Analysis

SPSS was used for statistical analysis, and the findings are reported as the means and standard deviations. A P-value < 0.05 was considered statistically significant. The sample size was a convenient sample, which included all available cases; hence, no formal power estimate was possible. The intraclass correlation coefficient (ICC) was used to assess the agreement between the SIR, fossa intercondylar femur, ACL volume, TPAPD, and LCAPD values.

The normality of the SIR values was evaluated using the Shapiro-Wilk test. Independent t tests were used to compare SIR values based on categorical variables such as sex and knee side. A repeated-measures analysis of variance was used to compare SIR values in five distinct regions of interest (ROIs). Pearson correlation coefficients were used to determine the associations between tunnel aperture areas and SIRs.

Univariate regression analyses were carried out on all continuous variables to identify variables associated with the graft SIR value. Variables with P-values < 0.05 (significant associations) in the univariate analysis were entered into a multivariate regression model to identify potential risk factors related to high graft SIR. Moreover, age, sex, and physical activity are known as characteristics linked with graft healing; hence, they were also included in the multivariate model.

Studies have shown that the signal intensity ratio (SIR) of proximal graft reflects ACL graft healing: SIR < 4 is a sensitive indicator indicating graft healing [10]. Based on these findings, patients were categorized into two groups: those with an SIR ≥ 4 and those with an SIR < 4. Receiver operating characteristic (ROC) curves for independent relevant factors were used to predict sensitivity, specificity, and cutoff values. An AUC value of 0.7 to 0.8 was considered good, whereas an AUC

value of 0.8 to 0.9 was considered exceptional. The sensitivity and specificity were balanced to obtain the cutoff value.

3. Results

The data are presented as the means ± SDs. Bold indicates $P < 0.05$. PTAPD: proximal tibia anterior-posterior distance; LCAPD: lateral femoral condylar anterior-posterior distance; MRI: magnetic resonance imaging; FIF: fossa intercondylar femur.

Table 1. Patient demographics and personal characteristics of male and female patients.

Characteristics	Total (54)	Male (45)	Female (9)	P-value
Age at the time of				
Surgery, y	28.65 ± 7.349	28.44 ± 7.04	29.67 ± 9.15	0.653
MRI, y	30.65 ± 7.349	30.44 ± 7.04	31.67 ± 9.15	0.653
Time from				
Injury to surgery, wk	11.748 ± 23.459	11.10 ± 24.37	14.95 ± 19.11	0.658
Surgery to MRI, mo	23.865 ± 1.968	23.86 ± 2.10	23.84 ± 1.17	0.976
Tunnel size, mm				
Femoral	54.746 ± 5.012	55.47 ± 4.59	51.09 ± 5.67	0.054
Tibial	54.578 ± 5.335	55.27 ± 5.04	51.09 ± 5.67	**0.030**
Aperture area, mm^2				
Femoral	64.705 ± 10.420	63.19 ± 7.32	72.23 ± 18.65	0.188
Tibial	60.444 ± 12.198	61.13 ± 12.82	57.00 ± 8.03	0.359
Volume, cm^3				
FIF	6.325 ± 0.862	6.37 ± 0.88	6.07 ± 0.76	0.315
Graft	4.465 ± 0.714	4.50 ± 0.73	4.26 ± 0.61	0.364
Distance, cm				
PTAPD	4.201 ± 0.498	4.33 ± 0.39	3.53 ± 0.43	**0.001**
LCAPD	6.123 ± 0.416	6.20 ± 0.40	5.70 ± 0.18	**0.001**
LCAPD-PTAPD ratio	1.475 ± 0.188	1.44 ± 0.16	1.63 ± 0.20	**0.005**

Two-year MRI was performed 23.86 ± 1.96 months after surgery, with a mean age of 28.65 ± 7.34 years. Table 1 displays the characteristics of the participants, including descriptive and operative data. The ICC index of interobserver reliability was 0.92 for the graft SIR value and 0.88 for the fossa intercondylar femur assessment. For the graft SIR value, the ICC index of intraobserver reliability was 0.90, whereas for the fossa intercondylar femur, it was 0.94. The ICC index of interobserver reliability for the ACL graft volume assessment was 0.85, whereas the

LCAPD/PTAPD ratio was 0.82. The intraobserver reliability ICCs for the ACL graft volume and the LCAPD/PTAPD ratio were 0.79 and 0.89, respectively.

The signal intensity ratio (SIR) was calculated by comparing the graft signal intensity to that of the posterior cruciate ligament (PCL). The MRI analysis included 54 individuals (16.6% of whom were female). Most patients had grafts with higher signal intensity than the PCL, as evidenced by SIR values greater than one.

The mean SIR values for the five graft regions were as follows: femoral aperture, 3.70 ± 1.05; proximal, 3.30 ± 1.22; middle, 3.11 ± 1.26; distal, 2.64 ± 0.90; and tibial aperture, 2.70 ± 0.83. Notably, the SIR in the femoral aperture was significantly greater than that in the distal and tibial aperture areas ($P < 0.001$). Similarly, the SIR in the proximal area was greater than that in the distal and tibial apertures ($P < 0.001$ and 0.003, respectively).

There were no significant differences in the mean graft SIR values between male and female patients throughout the five regions. The femoral aperture had an SIR of 3.63 ± 1.00 in males and 4.04 ± 1.28 in females ($P = 0.288$). In the proximal area, males had an SIR of 3.30 ± 1.28, whereas females had an SIR of 3.27 ± 0.96 ($P = 0.938$). The SIR in the middle area was 3.14 ± 1.35 for males and 2.99 ± 0.76 for females ($P = 0.746$). The SIR in the distal area was 2.67 ± 0.90 in males and 2.45 ± 0.97 in females ($P = 0.506$). At the tibial aperture, men had an SIR of 2.79 ± 0.85, whereas females had an SIR of 2.24 ± 0.55 ($P = 0.075$).

However, no significant changes in the mean graft SIR values were observed between the right and left sides. The mean femoral aperture SIR was 3.61 ± 1.01 on the right side and 3.79 ± 1.09 on the left ($P = 0.515$). In the proximal area, the right side had a mean score of 3.37 ± 1.11, whereas the left side had a mean score of 3.22 ± 1.35 ($P = 0.662$). In the center region, the right side had a value of 3.12 ± 1.42, whereas the left side had 3.11 ± 1.11. ($P = 0.971$). On the distal side, the mean score of the right side was 2.68 ± 1.02, whereas that of the left side was 2.59 ± 0.78 ($P = 0.732$). Finally, the right side had a mean tibial aperture SIR of 2.76 ± 0.92, whereas the left side had 2.63 ± 0.74 ($P = 0.583$).

Tunnel widening was detected in both the femoral and tibial tunnels, with a significantly greater increase in the femoral tunnel ($P < 0.001$) than in the tibial tunnel ($P = 0.001$).

The data are presented as coefficient B (P-value). Bolded P-values < 0.05 indicate statistically significant associations between variables and SIRs. PTAPD: proximal tibial anterior-posterior distance; LCAPA: lateral femoral condylar anterior-posterior distance; MRI: magnetic resonance imaging; FIF: fossa intercondylar femur; F. aperture, femoral aperture; T. aperture, tibial aperture.

Univariate regression analysis revealed that fossa intercondylar femur ($P = 0.001$), graft volume ($P = 0.028$), and LCAPD ($P = 0.044$) were significantly associated with the femoral aperture SIR value; femoral tunnel size ($P = 0.002$), tibial tunnel size ($P = 0.003$), femoral tunnel aperture area ($P = 0.032$), fossa intercondylar femur ($P < 0.001$), graft volume ($P = 0.033$), PTAPD ($P = 0.002$), LCAPD ($P = 0.040$), and the LCAPD/PTAPD ratio ($P = 0.026$) were significantly associated

with proximal graft SIR; femoral tunnel size (P = 0.007), tibial tunnel size (P = 0.013), femoral tunnel aperture area (P = 0.042), tibial aperture area (P = 0.048), fossa intercondylar femur (P < 0.001), PTAPD (P = 0.001), and the LCAPD/PTAPD ratio (P = 0.001) were significantly associated with middle graft SIRs (see Table 2).

Table 2. Univariate regression analysis of specific ROIs.

			Intra-articular		
Variables	F. Aperture	Proximal	Middle	Distal	T. aperture
Age at the time of					
Surgery, y	−0.154 (0.268)	0.015 (0.916)	−0.140 (0.314)	−0.243 (0.077)	0.005 (0.974)
MRI, y	−0.154 (0.268)	0.015 (0.916)	−0.140 (0.314)	−0.243 (0.77)	−0.005 (0.974)
Time from					
Injury to surgery, wk	−0.139 (0.316)	−0.137 (0.322)	−0.139 (0.318)	−0.151 (0.276)	0.009 (0.951)
Surgery to MRI, mo	0.064 (0.647)	0.168 (0.225)	0.039 (0.780)	0.108 (0.436)	−0.178 (0.197)
Tunnel size, mm					
Femoral	−0.261 (0.057)	−0.415 **(0.002)**	−0.362 **(0.007)**	−0.241 (0.079)	−0.094 (0.498)
Tibial	−0.197 (0.153)	−30.129 **(0.003)**	−0.335 **(0.013)**	−0.265 (0.053)	−0.166 (0.230)
Aperture area, mm^2					
Femoral	0.244 (0.075)	0.292 **(0.032)**	0.278 **(0.042)**	0.327 **(0.016)**	0.193 (0.162)
Tibial	0.052 (0.710)	0.057 (0.684)	0.270 **(0.048)**	0.132 (0.341)	0.418 **(0.002)**
Volume, cm^3					
FIF	−0.523 **(0.001)**	−0.807 **(0.001)**	−0.680 **(0.001)**	−0.546 **(0.001)**	−0.251 **(0.048)**
Graft	0.299 **(0.028)**	0.291 **(0.033)**	0.160 (0.246)	0.195 (0.158)	0.073 (0.600)
Distance, cm					
PTAPD	**−0.584 (0.095)**	−10.213 **(0.002)**	−10.402 **(0.001)**	−0.846 **(0.004)**	−0.615 **(0.026)**
LCAPD	0.762 **(0.044)**	0.878 **(0.040)**	0.795 **(0.066)**	0.833 **(0.009)**	0.319 (0.290)
LCAPD-PTAPD ratio	0.004 **(0.961)**	0.198 **(0.026)**	0.638 **(0.001)**	0.063 **(0.356)**	0.117 **(0.059)**

The data are presented in Exp(B) (P-value). Bolded P-values < 0.05 indicate an independent factor related to high SIRs. PTAPD: proximal tibial anterior-posterior distance; LCAPA: lateral femoral condylar anterior-posterior distance; FIF: fossa intercondylar femur (see Table 3).

Multivariate regression analysis revealed two significant predictors of high graft SIRs in the femoral aperture area: the fossa intercondylar femur (P = 0.009) and the LCAPD/PTAPD ratio (P = 0.005). Similarly, in the proximal area, the fossa intercondylar femur (P = 0.011) and the LCAPD/PTAPD ratio (P = 0.009) significantly contributed. Furthermore, the LCAPD/PTAPD ratio was a significant predictor of high graft SIRs for the middle section (P = 0.014).

Table 3. Multivariate regression analysis for factors related to SIR values at specific ROIs.

Variables	F. Aperture	Proximal	Middle	Distal	T. Aperture
Age at the time of surg.	0.937 (0.235)	1.079 (0.328)	1.041 (0.586)	0.881 (0.241)	1.077 (0.188)
Sex	0.876 (0.923)	0.038 (0.215)	0.482 (0.715)	0.479 (0.813)	0.768 (0.873)
Tunnel size, mm					
Femoral	0.703 (0.768)	0.572 (0.791)	0.906 (0.929)	0.009 (0.867)	0.942 (0.439)
Tibial	1.263 (0.845)	1.178 (0.938)	1.084 (0.942)	98.612 (0.870)	0.890 (0.135)
Volume, cm^3					
FIF	0.150 **(0.009)**	0.151 **(0.011)**	1.342 (0.599)	0.361 (0.100)	0.998 (0.998)
Graft	2.291 (0.147)	1.681 (0.609)	0.568 (0.378)	3.889 (0.234)	1.928 (0.369)
Distance, cm					
LCAPD	2.857 (0.286)	10.856 (0.097)	3.318 (0.462)	30.825 (0.144)	0.301 (0.401)
PTAPD	3.265 (0.355)	22.075 (0.803)	1.121 (0.873)	0.045 (0.468)	0.120 (0.385)
LCAPD-PTAPD ratio	673.425 **(0.005)**	2123.150 **(0.009)**	317.472 **(0.014)**	0.805 (0.727)	5.966 (0.395)

In the proximal section of the intraarticular graft, a cutoff LCAPD/TPAPD ratio of 1.50 had a sensitivity of 87.5% and specificity of 68.4% for poor graft healing (AUC of 0.85), as well as 72.2% sensitivity and 63.9% specificity for poor graft healing at the femoral aperture (AUC of 0.72). A cutoff FIF of 6.2 in the proximal region had a sensitivity of 81.6% and a specificity of 75% for good graft healing (AUC of 0.84), as did 77.8% sensitivity and 61.1% specificity (AUC of 0.73).

4. Discussion

This study aimed to analyze the magnetic resonance imaging changes of graft healing 2 years following anterior cruciate ligament reconstruction and identify independent factors associated with poor ACL graft healing. Importantly, the signal intensity of the reconstructed graft was greater than that of the PCL. Furthermore, the LCAPD/PTAPD ratio and the fossa intercondylar femur were found to be independent factors associated with poor graft healing outcomes.

Most ACL grafts have shown high signal intensity two years after surgery, indicating ongoing healing and remodeling, which is crucial for the success of the procedure in restoring knee stability and function. This aligns with prior research that showed similar graft maturation patterns [20] [21]. The SIR in the femoral aperture of the ACL grafts was significantly greater than that in the distal and tibial aperture areas. Similarly, the SIR in the proximal area was greater than that in the distal region and tibial aperture. The difference may be due to the greater vascular supply and cellular activity in the femoral tunnel and proximal regions than in the distal and tibial tunnel regions, which is essential for optimal graft integration and healing processes. These findings contribute to the existing evidence indicating that the proximal femoral region of the intra-articular graft may be the most important region for complete graft healing [22]. Previous studies have used MRI to analyze

ACL reconstruction graft changes and have shown a greater signal intensity ratio in the proximal region and within the femoral tunnel area [23]. Furthermore, these studies revealed that tunnel widening is more severe in the femur than in the tibia [24]. Putnis *et al.* [23] aimed to establish whether a hamstring tendon autograft for ACLR changes in appearance on MRI after 1 or 2 years, and whether this change affects a patient's ability to return to sports. This study showed that the graft SIR of the femoral aperture was considerably greater than that of the tibial aperture.

In contrast, the SNQ of 24 patients who underwent primary ACL reconstruction via an autologous quadriceps tendon and a bone plug was measured in three different locations (proximal, mid-substance, and distal), and after 24 months, no significant differences were detected among the three regions [18].

Three phases of ACL graft ligamentization have been described, corresponding to the observed structural changes [25]: early (healing), remodeling, and maturation. Although the general sequence of these phases is widely accepted in literature, their duration is debated. Although Scheffler *et al.* [26] observed that ACL graft maturation is nearly complete at six months, others have described the process as lasting two to four years postoperatively [27] or even longer for complete graft maturity [28]. In a comprehensive literature review on return to play after ACL reconstruction, Barber-Westin and Noyes [29] found that in 32% of the studies, time after surgery was the sole factor used to determine whether patients could return to sports. However, it was determined that this criterion alone was insufficient, which is plausible considering the variety of reported graft maturation durations. MRI is a non-invasive alternative [3] [30]. Using routine MRI sequences, a low signal in the graft, similar to that observed in the native PCL, has been proposed to indicate advanced maturation [3]. In contrast, hyperintense signals in the graft have been associated with inferior biomechanical properties and hypervascular/hypercellular reparative tissues [30]. However, subjective outcome and clinical examination of knee laxity remain important to assess the treatment success and to allow to return to sports.

Waltz *et al.* [31] reported a variable correlation between MRI graft appearances and arthroscopic evaluation of the graft. Lutz *et al.* [3] discovered no association between ACL MRI graft signal and clinical outcome scores or KT-1000 measurements over two years.

Two independent factors were associated with high SIR values in this current study: the LCAPD/PTAPD ratio (particularly in the femoral aperture, proximal, and middle regions) and the fossa intercondylar femur (in the proximal region and femoral tunnel area). These findings offer valuable insights into the role of anatomical and structural factors in graft healing and their potential relationship with long-term outcomes after ACL reconstruction. However, we did not observe any significant sex differences in graft signal intensity, indicating that biological factors related to sex may not significantly influence graft healing at two years post-surgery. Similarly, the side of surgery (right vs. left knee) did not significantly af-

fect graft healing, suggesting that surgical techniques and other patient-specific factors may play a more substantial role in determining graft outcomes. Notably, a high LCAPD/PTAPD ratio may increase mechanical stress on the graft, potentially impeding its healing. This finding indicates that the alignment and positioning of the femoral and tibial components, as indicated by the LCAPD/PTAPD ratio, are important factors in graft healing. These findings are consistent with those of previous studies:

Misir *et al.* aimed to determine individual anatomic parameters that are independently related to ACL rupture and their diagnostic value. They discovered that the LCAPD/TPAPD ratio may be utilized to differentiate between patients at risk of ACL rupture and those who are not [32] [33].

Other studies have similarly highlighted the significance of the graft position in ACL outcomes. For instance, Kazemi *et al.* [34] showed that inadequate graft placement, particularly at the femoral or tibial tunnel site, negatively impacts ACL reconstruction outcomes, such as rerupture rates and MRI signal intensity.

The small-fossa intercondylar femur was also revealed to be a factor associated with high SIR values in both the proximal and femoral tunnel areas. These findings are consistent with those of SE. Putnis *et al.* [10] One-year postoperative MRI was used to assess the graft of hamstring autograft ACL reconstruction (ACLR) and identify individuals at high risk of graft rupture. The proximal region of the ACL graft may have high signal intensity, which is connected to the likelihood of graft failure and might be impacted by the fossa intercondylar femur (notch volume). The fossa intercondylar femur is an important anatomical feature in ACL reconstruction, and its size can have several ramifications for the effectiveness of the surgery, particularly in terms of graft healing and overall results [35]. Because it is intimately engaged in the graft insertion location and integration into the femoral tunnel, the closeness and fit of the graft within the fossa intercondylar femur have been identified as key parameters influencing biological healing and mechanical performance [36].

Park *et al.* [37] determined the relationship between patient-specific geometric factors and tunnel placement in graft impingement, and the MRI signal intensity of ACL grafts was used. They discovered that a low notch was a more significant contributing factor to increased signal intensities of the ACL graft and recommended a more focused approach on intercondylar notch anatomy during tibial tunnel placement to avoid roof impingement.

In contrast, Moon *et al.* reported that the surgical results of anatomical single-bundle ACL reconstruction in patients with relatively small intercondylar notch volumes were comparable to those in patients with large notch volumes [38]. Although still debatable, a small intercondylar notch is generally recognized as a possible risk factor for ACL injuries [39] [40].

Putnis *et al.* [41] discovered that graft impingement was more common in cases when the graft size exceeded the dimensions of the femoral notch. This suggests that larger grafts may be more susceptible to impingement, which could explain the

high SIR found in our study. Furthermore, Tashiro *et al.* [18] found that graft bending angles and tunnel orientation have a substantial impact on early graft healing, with larger grafts likely leading to poor positioning and higher signal intensity.

The anatomical risk factors identified in this study, including the LCAPD/PTAPD ratio and the size of the fossa intercondylar femur, have significant clinical implications. Surgeons can optimize surgical techniques to improve graft alignment and positioning, thereby enhancing the LCAPD/PTAPD ratio. Rehabilitation strategies can be tailored based on the size of the FIF to ensure conservative management and optimal graft healing.

5. Conclusion

This study demonstrated that most grafts presented elevated signal intensity, particularly in the femoral and proximal regions, indicating ongoing healing and remodeling. A larger LCAPD/PTAPD ratio and a smaller fossa intercondylar femur were identified as independent factors associated with poorer or delayed ACL graft healing.

6. Limitations and Future Directions

While this study provides valuable insights into the factors influencing ACL graft healing, it is important to note several limitations. The relatively small sample size and retrospective nature of the study, which is subject to some limitations such as selection bias, missing data, and lack of randomization, may limit the generalizability of our findings. Furthermore, the use of a single imaging modality may not adequately represent the complex biological processes involved in graft recovery.

Future studies should aim to address these limitations through larger sample sizes, prospective designs, and the inclusion of multiple imaging modalities to provide a more comprehensive understanding of ACL graft healing.

Acknowledgements

I extend my heartfelt thanks to my professor, Quan Zhou, for his guidance and expertise. To the faculty and staff at Southern Medical University, thank you for providing the resources that made this work possible.

Conflicts of Interest

The authors declare no conflicts of interest.

References

[1] Boyd, E., Endres, N.K. and Geeslin, A.G. (2024) Postoperative Healing and Complications Based on Anterior Cruciate Ligament Reconstruction Graft Type. *Annals of Joint*, **9**, 30. https://doi.org/10.21037/aoj-24-3

[2] Bolia, I.K., Haratian, A., Bell, J.A., Hasan, L.K., Saboori, N., Palmer, R., *et al.* (2021) Managing Perioperative Pain after Anterior Cruciate Ligament (ACL) Reconstruction: Per-

spectives from a Sports Medicine Surgeon. *Open Access Journal of Sports Medicine*, **12**, 129-138. https://doi.org/10.2147/oajsm.s266227

[3] Lutz, P.M., Achtnich, A., Schütte, V., Woertler, K., Imhoff, A.B. and Willinger, L. (2021) Anterior Cruciate Ligament Autograft Maturation on Sequential Postoperative MRI Is Not Correlated with Clinical Outcome and Anterior Knee Stability. *Knee Surgery, Sports Traumatology, Arthroscopy*, **30**, 3258-3267. https://doi.org/10.1007/s00167-021-06777-4

[4] Ong, M.T., Lu, X., Choi, B.C., Wan, S., Wang, Q., Man, G.C., *et al.* (2024) Vitamin D as an Intervention for Improving Quadriceps Muscle Strength in Patients after Anterior Cruciate Ligament Reconstruction: Study Protocol for a Randomized Double-Blinded, Placebo-Controlled Clinical Trial. *Trials*, **25**, Article No. 251. https://doi.org/10.1186/s13063-024-08094-w

[5] Shanmugaraj, A., Mahendralingam, M., Gohal, C., Horner, N., Simunovic, N., Musahl, V., *et al.* (2020) Press-Fit Fixation in Anterior Cruciate Ligament Reconstruction Yields Low Graft Failure and Revision Rates: A Systematic Review and Meta-Analysis. *Knee Surgery, Sports Traumatology, Arthroscopy*, **29**, 1750-1759. https://doi.org/10.1007/s00167-020-06173-4

[6] Biercevicz, A.M., Murray, M.M., Walsh, E.G., Miranda, D.L., Machan, J.T. and Fleming, B.C. (2013) T_2* MR Relaxometry and Ligament Volume Are Associated with the Structural Properties of the Healing ACL. *Journal of Orthopaedic Research*, **32**, 492-499. https://doi.org/10.1002/jor.22563

[7] Li, H., Chen, J., Li, H., Wu, Z. and Chen, S. (2016) MRI-Based ACL Graft Maturity Does Not Predict Clinical and Functional Outcomes during the First Year after ACL Reconstruction. *Knee Surgery, Sports Traumatology, Arthroscopy*, **25**, 3171-3178. https://doi.org/10.1007/s00167-016-4252-5

[8] Biercevicz, A.M., Miranda, D.L., Machan, J.T., Murray, M.M. and Fleming, B.C. (2013) *In Situ*, Noninvasive, T_2*-Weighted MRI-Derived Parameters Predict *ex Vivo* Structural Properties of an Anterior Cruciate Ligament Reconstruction or Bioenhanced Primary Repair in a Porcine Model. *The American Journal of Sports Medicine*, **41**, 560-566. https://doi.org/10.1177/0363546512472978

[9] Kiapour, A.M., Ecklund, K., Murray, M.M., Flutie, B., Freiberger, C., Henderson, R., *et al.* (2019) Changes in Cross-Sectional Area and Signal Intensity of Healing Anterior Cruciate Ligaments and Grafts in the First 2 Years after Surgery. *The American Journal of Sports Medicine*, **47**, 1831-1843. https://doi.org/10.1177/0363546519850572

[10] Putnis, S.E., Oshima, T., Klasan, A., Grasso, S., Neri, T., Fritsch, B.A., *et al.* (2021) Magnetic Resonance Imaging 1 Year after Hamstring Autograft Anterior Cruciate Ligament Reconstruction Can Identify Those at Higher Risk of Graft Failure: An Analysis of 250 Cases. *The American Journal of Sports Medicine*, **49**, 1270-1278. https://doi.org/10.1177/0363546521995512

[11] Li, H., Chen, S., Tao, H., Li, H. and Chen, S. (2014) Correlation Analysis of Potential Factors Influencing Graft Maturity after Anterior Cruciate Ligament Reconstruction. *Orthopaedic Journal of Sports Medicine*, **2**, Article ID: 2325967114553552.

[12] van Eck, C.F., Schkrohowsky, J.G., Working, Z.M., Irrgang, J.J. and Fu, F.H. (2012) Prospective Analysis of Failure Rate and Predictors of Failure after Anatomic Anterior Cruciate Ligament Reconstruction with Allograft. *The American Journal of Sports Medicine*, **40**, 800-807. https://doi.org/10.1177/0363546511432545

[13] Grasso, S., Linklater, J., Li, Q. and Parker, D.A. (2018) Validation of an MRI Protocol for Routine Quantitative Assessment of Tunnel Position in Anterior Cruciate Ligament Reconstruction. *The American Journal of Sports Medicine*, **46**, 1624-1631.

https://doi.org/10.1177/0363546518758950

[14] Hakozaki, A., Niki, Y., Enomoto, H., Toyama, Y. and Suda, Y. (2015) Clinical Significance of T_2*-Weighted Gradient-Echo MRI to Monitor Graft Maturation over One Year after Anatomic Double-Bundle Anterior Cruciate Ligament Reconstruction: A Comparative Study with Proton Density-Weighted MRI. *The Knee*, **22**, 4-10. https://doi.org/10.1016/j.knee.2014.11.004

[15] Retzky, J.S., Chipman, D.E., Mintz, D.N., Cordasco, F.A. and Green, D.W. (2024) Association of Lateral Extra-Articular Tenodesis with Improved Graft Maturity on MRI 2 Years after ACL Reconstruction with Quadriceps Tendon Autograft in Skeletally Immature Athletes. *Orthopaedic Journal of Sports Medicine*, **12**, 1-10. https://doi.org/10.1177/23259671231211885

[16] Oshima, T., Putnis, S., Grasso, S., Klasan, A. and Parker, D.A. (2019) Graft Size and Orientation within the Femoral Notch Affect Graft Healing at 1 Year after Anterior Cruciate Ligament Reconstruction. *The American Journal of Sports Medicine*, **48**, 99-108. https://doi.org/10.1177/0363546519885104

[17] Pauvert, A., Robert, H., Gicquel, P., Graveleau, N., Pujol, N., Chotel, F., *et al.* (2018) MRI Study of the Ligamentization of ACL Grafts in Children with Open Growth Plates. *Orthopaedics & Traumatology*: *Surgery & Research*, **104**, S161-S167. https://doi.org/10.1016/j.otsr.2018.09.003

[18] Tashiro, Y., Gale, T., Sundaram, V., Nagai, K., Irrgang, J.J., Anderst, W., *et al.* (2017) The Graft Bending Angle Can Affect Early Graft Healing after Anterior Cruciate Ligament Reconstruction: *In Vivo* Analysis with 2 Years' Follow-Up. *The American Journal of Sports Medicine*, **45**, 1829-1836. https://doi.org/10.1177/0363546517698676

[19] Zhang, C., Xie, G., Dong, S., Chen, C., Peng, X., Yuan, F., *et al.* (2019) A Novel Morphological Classification for the Femoral Notch Based on MRI: A Simple and Effective Assessment Method for the Femoral Notch. *Skeletal Radiology*, **49**, 75-83. https://doi.org/10.1007/s00256-019-03255-4

[20] Chu, C.R. and Williams, A.A. (2019) Quantitative MRI UTE-T_2* and T_2* Show Progressive and Continued Graft Maturation over 2 Years in Human Patients after Anterior Cruciate Ligament Reconstruction. *Orthopaedic Journal of Sports Medicine*, **7**, 1-10. https://doi.org/10.1177/2325967119863056

[21] Warth, R.J., Zandiyeh, P., Rao, M., Gabr, R.E., Tashman, S., Kumaravel, M., *et al.* (2020) Quantitative Assessment of *in Vivo* Human Anterior Cruciate Ligament Autograft Remodeling: A 3-Dimensional UTE-T_2* Imaging Study. *The American Journal of Sports Medicine*, **48**, 2939-2947. https://doi.org/10.1177/0363546520949855

[22] Putnis, S., Klasan, A., Oshima, T., Grasso, S., Coolican, M., Fritsch, B., *et al.* (2020) High Signal on MRI at the Femoral Tunnel Aperture after 1-Year Increases Risk of Subsequent Graft Rupture—An Analysis of 250 Cases. *The Knee*, **27**, S24. https://doi.org/10.1016/j.knee.2020.07.058

[23] Putnis, S.E., Klasan, A., Oshima, T., Grasso, S., Neri, T., Coolican, M.R.J., *et al.* (2022) Magnetic Resonance Imaging Assessment of Hamstring Graft Healing and Integration 1 and Minimum 2 Years after ACL Reconstruction. *The American Journal of Sports Medicine*, **50**, 2102-2110. https://doi.org/10.1177/03635465221096672

[24] Mayr, R., Smekal, V., Koidl, C., Coppola, C., Fritz, J., Rudisch, A., *et al.* (2017) Tunnel Widening after ACL Reconstruction with Aperture Screw Fixation or All-Inside Reconstruction with Suspensory Cortical Button Fixation: Volumetric Measurements on CT and MRI Scans. *The Knee*, **24**, 1047-1054. https://doi.org/10.1016/j.knee.2017.06.007

[25] Pauzenberger, L., Syré, S. and Schurz, M. (2013) "Ligamentization" in Hamstring Tendon Grafts after Anterior Cruciate Ligament Reconstruction: A Systematic Review of

the Literature and a Glimpse into the Future. *Arthroscopy: The Journal of Arthroscopic & Related Surgery*, **29**, 1712-1721. https://doi.org/10.1016/j.arthro.2013.05.009

[26] Scheffler, S.U., Unterhauser, F.N. and Weiler, A. (2008) Graft Remodeling and Ligamentization after Cruciate Ligament Reconstruction. *Knee Surgery, Sports Traumatology, Arthroscopy*, **16**, 834-842. https://doi.org/10.1007/s00167-008-0560-8

[27] Falconiero, R., DiStefano, V. and Cook, T. (1998) Revascularization and Ligamentization of Autogenous Anterior Cruciate Ligament Grafts in Humans. *Arthroscopy: The Journal of Arthroscopic & Related Surgery*, **14**, 197-205. https://doi.org/10.1016/s0749-8063(98)70041-6

[28] Janssen, R.P.A., van der Wijk, J., Fiedler, A., Schmidt, T., Sala, H.A.G.M. and Scheffler, S.U. (2011) Remodelling of Human Hamstring Autografts after Anterior Cruciate Ligament Reconstruction. *Knee Surgery, Sports Traumatology, Arthroscopy*, **19**, 1299-1306. https://doi.org/10.1007/s00167-011-1419-y

[29] Barber-Westin, S.D. and Noyes, F.R. (2011) Factors Used to Determine Return to Unrestricted Sports Activities after Anterior Cruciate Ligament Reconstruction. *Arthroscopy: The Journal of Arthroscopic & Related Surgery*, **27**, 1697-1705. https://doi.org/10.1016/j.arthro.2011.09.009

[30] Grassi, A., Bailey, J.R., Signorelli, C., Carbone, G., Wakam, A.T., Lucidi, G.A., *et al.* (2016) Magnetic Resonance Imaging after Anterior Cruciate Ligament Reconstruction: A Practical Guide. *World Journal of Orthopedics*, **7**, 638-649. https://doi.org/10.5312/wjo.v7.i10.638

[31] Waltz, R.A., Solomon, D.J. and Provencher, M.T. (2014) A Radiographic Assessment of Failed Anterior Cruciate Ligament Reconstruction: Can Magnetic Resonance Imaging Predict Graft Integrity? *The American Journal of Sports Medicine*, **42**, 1652-1660. https://doi.org/10.1177/0363546514532335

[32] Misir, A., Uzun, E., Sayer, G., Guney, B. and Guney, A. (2022) Anatomic Factors Associated with the Development of an Anterior Cruciate Ligament Rerupture in Men: A Case-Control Study. *The American Journal of Sports Medicine*, **50**, 3228-3235. https://doi.org/10.1177/03635465221120378

[33] Misir, A., Sayer, G., Uzun, E., Guney, B. and Guney, A. (2022) Individual and Combined Anatomic Risk Factors for the Development of an Anterior Cruciate Ligament Rupture in Men: A Multiple Factor Analysis Case-Control Study. *The American Journal of Sports Medicine*, **50**, 433-440. https://doi.org/10.1177/03635465211062594

[34] Kazemi, S.M., *et al.* (2017) Comparison of Clinical Outcomes between Different Femoral Tunnel Positions after Anterior Cruciate Ligament Reconstruction Surgery. *The Archives of Bone and Joint Surgery*, **5**, 419-425.

[35] Hirtler, L., Kainberger, F. and Röhrich, S. (2021) The Intercondylar Fossa—A Narrative Review. *Clinical Anatomy*, **35**, 2-14. https://doi.org/10.1002/ca.23773

[36] Moon, H., Choi, C., Yoo, J., Jung, M., Lee, T., Choi, K., *et al.* (2021) The Graft Insertion Length in the Femoral Tunnel during Anterior Cruciate Ligament Reconstruction with Suspensory Fixation and Tibialis Anterior Allograft Does Not Affect Surgical Outcomes but Is Negatively Correlated with Tunnel Widening. *Arthroscopy: The Journal of Arthroscopic & Related Surgery*, **37**, 2903-2914.e1. https://doi.org/10.1016/j.arthro.2021.03.072

[37] Park, S.Y., Cho, J.H., Ho, J.P.Y., Tu, N.T., Kim, Y.B. and Lee, Y.S. (2023) Graft Impingement Increases Anterior Cruciate Ligament Graft Signal More than Acute Graft Bending Angle: Magnetic Resonance Imaging-based Study in Outside-in Anterior Cruciate Ligament Reconstruction. *Knee Surgery, Sports Traumatology, Arthroscopy*, **31**, 4379-4389. https://doi.org/10.1007/s00167-023-07491-z

[38] Moon, H., Choi, C., Jung, M., Yoo, J., Kwon, H., Hong, Y., *et al.* (2024) Small Intercondylar Notch Size Is Not Associated with Poor Surgical Outcomes of Anatomical Single-Bundle Anterior Cruciate Ligament Reconstructions. *Clinics in Orthopedic Surgery*, **16**, Article No. 73. https://doi.org/10.4055/cios23081

[39] Iriuchishima, T., Goto, B. and Fu, F.H. (2020) Truncated-Pyramid Shape Simulation for the Measurement of Femoral Intercondylar Notch Volume Can Detect the Volume Difference between ACL-Injured and Intact Subjects. *Knee Surgery, Sports Traumatology, Arthroscopy*, **29**, 1709-1713. https://doi.org/10.1007/s00167-020-06204-0

[40] Jha, V. and Pandit, A. (2021) Notch Volume Measured on Magnetic Resonance Imaging Is Better than 2-Dimensional Notch Parameters for Predicting Noncontact Anterior Cruciate Ligament Injury in Males. *Arthroscopy: The Journal of Arthroscopic & Related Surgery*, **37**, 1534-1543.e1. https://doi.org/10.1016/j.arthro.2020.11.050

[41] Putnis, S., Neri, T., Grasso, S., Linklater, J., Fritsch, B. and Parker, D. (2019) ACL Hamstring Grafts Fixed Using Adjustable Cortical Suspension in Both the Femur and Tibia Demonstrate Healing and Integration on MRI at One Year. *Knee Surgery, Sports Traumatology, Arthroscopy*, **28**, 906-914. https://doi.org/10.1007/s00167-019-05556-6